

Low Elastic Modulus and High Charge Mobility of Low-Crystallinity Indacenodithiophene-Based Semiconducting Polymers for Potential **Applications in Stretchable Electronics**

Yilin Li, Wesley K. Tatum, Jonathan W. Onorato, Yongcao Zhang, and Christine K. Luscombe*,†,‡,§

[†]Department of Materials Science & Engineering, [‡]Department of Chemistry, and [§]Molecular Engineering & Sciences Institute, University of Washington, Seattle, Washington 98195, United States

Supporting Information

ABSTRACT: A series of alkyl-substituted indacenodithiophene (alkyl-IDT) semiconducting donor-acceptor polymers were designed by DFT to have varying degrees of backbone planarity and synthesized via direct arylation polymerization (DArP). These polymers exhibit weak intermolecular interactions, a glass transition temperature (T_g) below room temperature, and low degrees of crystallinity from XRD measurements. Despite this, the field-effect mobilities (μ) of these polymers are relatively high (0.06-0.20 cm² V⁻¹ s⁻¹) with mobility increasing with increasing backbone planarity. Because of the weak intermolecular

interactions, the polymers exhibit low elastic moduli (E_f) of less than 450 MPa. The polymer with the most twisted backbone exhibits high ductility with a crack-onset strain (CoS) over 100%. These structure-property relationship studies provide useful guidelines for designing semiconducting polymers with high mobility, low stiffness, and high ductility enabling applications in stretchable electronics.

■ INTRODUCTION

In the past two decades, the field of semiconducting polymers has advanced significantly because of extensive research on organic photovoltaics (OPVs),1 organic field-effect transistors (OFETs),² organic light-emitting diodes (OLEDs),³ and organic thermoelectrics (OTEs).⁴ As a consequence, materials with excellent optical, electrical, and thermal properties have been developed. Recently, investigation of the mechanical properties of semiconducting polymers has increased, due in part to the emergence of biomedical devices for physiological monitoring,⁵ implanted treatments,⁶ electronic skin,⁷ and human-machine interfaces.8 Semiconducting polymers require mechanical compatibility with biological tissue to be suitable for bioelectronics applications. Traditional approaches that impart mechanical compliance to semiconducting devices are based on geometric designs, such as buckles,9 wavy patterns,5,6 and kirigami. 10 Increasingly, attention has been paid to semiconducting polymers with intrinsic mechanical compliance, largely due to the potential advantages of easier production, reduced constraints on large scale device design, higher device density, and improved strain tolerance. 11,12 In contrast to flexibility, which is the property of a material to withstand bending deformation, stretchability additionally includes deformation under tensile modes. Flexibility is easily achievable, as making a material thin is typically enough to impart flexibility. Achieving stretchability of semiconducting polymers is typically difficult because in most cases tensile

deformation results in permanent alterations to the microstructure, significantly affecting the charge transport properties. In spite of this, several approaches have been developed to address this issue. For example, noncovalent cross-linking in amorphous domains in semiconducting polymers can efficiently reduce the tensile force applied to crystal domains. 13 Nanoconfinement of semiconducting polymers in elastomers has also proven effective for achieving material ductility while maintaining the charge transport properties. 14,15 On a molecular level, the ductility of semiconducting polymers can also be achieved by backbone engineering, 16,1° modification 18,19 and random segmentation 20-22 modification, 18,19 and random segmentation.

In an effort to develop semiconducting polymers with intrinsically high ductility (in other words, designing fully π conjugated stretchable polymers), reducing the π - π intermolecular interactions between polymer chains becomes important. Classical thinking is that crystalline domains are a necessity for high-mobility semiconducting polymers. However, the strong intermolecular interactions required for crystallinity are detrimental to mechanical properties since they reduce the ability of chains to slide past one another, reducing maximum elongation. ^{23,24} However, recent studies have shown that high crystallinity is not a requirement for high

Received: April 27, 2018 Revised: July 27, 2018 Published: August 10, 2018

mobility. Instead, local aggregates or small crystals separated by short distances are sufficient for high mobility.²⁵ Specifically, studies related to semiconducting copolymers containing alkyl-substituted indacenodithiophene (alkyl-IDT) have shown that high charge mobility of over 2.0 cm² V⁻¹ s⁻¹ can be achieved 26,27 while also having small crystallites with no preferential orientation, which could potentially enable reduced stiffness and high stretchability. The high charge mobility has been attributed to the efficient quasi-onedimensional charge transport attributed to the rigid polymer backbones in amorphous domains that connect the small crystallites. 25,28 Our own recent study has shown that through backbone engineering an alkyl-IDT-containing polymer could exhibit a low stiffness as well as high ductility, demonstrating an elastic modulus (E_f) of 200 MPa and a crack-onset strain (CoS) of 40%, properties that were achieved through reducing the strength of intermolecular interactions. ¹⁷ In light of these previous results, our current study investigates design criteria to achieve high-mobility, low-stiffness, and high-ductility semiconducting polymers, with a particular emphasis on the effects of intermolecular interactions.

Herein, we report a study of the structure—property relationships of a series of alkyl-IDT semiconducting donor—acceptor polymers. These polymers are designed to investigate the effects of an increasing backbone twist on the mechanical and electrical properties. They exhibit relatively high charge mobilities that range from 0.06 to 0.20 cm 2 V $^{-1}$ s $^{-1}$. These charge mobilities follow the general trend of increasing backbone planarity leading to increased mobility. The polymer thin films exhibit low stiffness, with $E_{\rm f}$ less than 450 MPa, a property that is partially attributed to the long, linear side chains emanating from a bridging C(sp 3). One polymer of the series exhibits extremely high ductility, with a CoS of over 100%, which is largely attributed to its kinked backbone conformation.

■ RESULTS AND DISCUSSION

Backbone Conformation. The chemical structures of three alkyl-IDT polymers (PIDTTPD, PIDTBTD, and PIDTBPD) are shown in Table 1. The backbone conformation is obtained from density functional theory (DFT) calculations. McCormick et al. previously suggested that the use of four repeating units for computing semiconducting copolymers can accurately represent the polymer saturation length, at which polymer structural and electronic properties exhibit minimal change by adding more repeating units.²⁹ In this study, to be thorough, structures with five repeating units have been calculated. To quantify the backbone conformation, three distinct dihedral angles are used. As depicted in Figure 1, dihedral angles exist between donor and acceptor units (ϕ_{DA}), between donor units (ϕ_{DD}) , and between acceptor units (ϕ_{AA}) . PIDTTPD possesses a perfectly planar backbone with all three dihedral angles equal to zero $(\phi_{\mathrm{DA}} = \phi_{\mathrm{DD}} = \phi_{\mathrm{AA}} = 0^{\circ}$, Figure S1a). This is due to the S-O interaction between the donor thiophene group and the acceptor carbonyl group, acting as a conformational lock.³⁰ There is a slight twist between the donor and acceptor units ($\phi_{DA} = 7.5^{\circ}$, Figure S1b) in the backbone of PIDTBTD while all the donor (or acceptor) units are essentially planar ($\phi_{\rm DD}=0.8^{\circ}$ and $\phi_{\rm AA}=0.4^{\circ}$). Significant twist between donor and acceptor units is found in the backbone of PIDTBPD ($\phi_{\rm DA}$ = 35.9°, Figure S1c). In addition, the donor units are not in the same plane ($\phi_{\rm DD}$ = 16.2°). Our previous study has suggested that the kinked

Table 1. Relevant Quantitative Results of the Polymers*

D - 1		DIDTTDD	DIDTDTD	DIDTDDD
Polymer name		PIDTTPD	PIDTBTD	PIDTBPD C14H30 C14H30
Chemical structure		C ₁₆ H ₃₃ C ₁₆ H ₃₃ O _N O	C16H22 C16H22 N.2.N	C ₁₆ H ₂₅ C ₁₆ H ₂₅ O _N O
DFT	ϕ_{DA}	0	7.5°	35.9°
	ϕ_{DD}	0	0.8°	16.2°
	ϕ_{AA}	0	0.4°	0.5°
Molecular weight	M _n , kg·mol⁻¹	14	15	15
information	Đ	1.6	1.7	1.7
UV-Vis and PL ^a	λ_{abs} , nm	604 (608)	645 (615)	502 (502)
	λ_{em} , nm	629 (647)	716 (725)	574 (569)
	⊿λ, nm	25 (39)	71 (110)	72 (67)
DSC	T_g , °C	-0.6	17.6	-8.1
$\begin{array}{c} \text{XRD} \\ (2\theta = 3.7^{\circ}) \end{array}$	I_0	1.98	1.82	1.23
	I	1.93	1.60	0.60
	$1-I/I_0$	3%	12%	51%
Charge transport properties	μ, cm ² ·V ⁻	0.20 ± 0.10	0.17 ± 0.09	0.06 ± 0.03
	I_{on}/I_{off}	$6 \times 10^4 \pm 3 \times 10^4$	$2 \times 10^4 \pm 2 \times 10^4$	$3 \times 10^6 \pm 2 \times 10^6$
Mechanical properties	E _f , MPa	110-410	150-360	80-400
	CoS	3%	3%	> 100%

** ϕ_{DA} : dihedral angle between donor and acceptor units; ϕ_{DD} : dihedral angle between donor units; ϕ_{AA} : dihedral angle between acceptor units; M_{n} : number-average molecular weight; D: dispersity; λ_{abs} : absorption maximum; λ_{em} : emission maximum; $\Delta \lambda$: Stokes shift; T_{g} : glass transition temperature; I_0 : intensity before annealing; I: intensity after annealing; $1 - I/I_0$: percentage of intensity change; μ : charge mobility; $I_{\mathrm{on}}/I_{\mathrm{off}}$: current on/off ratio; E_{f} : elastic modulus; CoS: crack-onset strain. "Numbers in parentheses represent polymer film results.

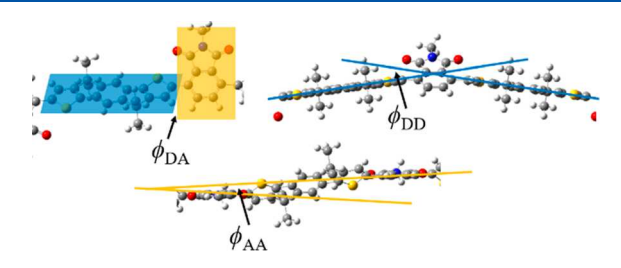


Figure 1. Definitions of the dihedral angles that are described in this work

backbone of PIDTBPD is due to the steric effects between the donor and acceptor units.¹⁷ These steric effects arose from the hydrogen atoms in the benzo group in the acceptor units in PIDTBPD. This disrupts the S–O interaction between the donor thiophene and the acceptor carbonyl group in PIDTBPD.

Polymer Synthesis. The synthesis of three alkyl-IDT polymers is depicted in Scheme 1. The synthetic route of the diBrTPD monomer is also shown in the scheme. The IDT and diBrBPD monomers were synthesized according to a previous report. The polymers were synthesized via DArP between the hydrogen-terminated donor unit (i.e., IDT) and bromineterminated acceptor unit (i.e., diBrTPD, diBrBTD, or diBrBPD).31,32 Employing the chemistry of DArP avoids prefunctionalization of monomers. From this, synthesis and purification are simplified, resulting in decreased costs for polymer synthesis.³³ For the syntheses of the three polymers, monomer molar ratios (donor:acceptor) of 1:1 for PIDTTPD, 1:1 for PIDTBTD, and 1:1.6 for PIDTBPD were used to achieve similar number-averaged molecular weight ($M_n = 14$ – 15 kg mol⁻¹) and dispersity (D = 1.6-1.7) (Table 1 and Figure S2). The purpose is to minimize the effects of molecular weight and dispersity on the polymer mechanical and electronic properties. The polymers exhibit structural defects

Scheme 1. Synthetic Routes of the Polymers and diBrTPD $Monomer^a$

"Reagents and conditions: (i, ii, and iii) $Pd_2(dba)_3$, P(o-anisyl)_3, Cs_2CO_3 , PivOH, o-xylene, 100 °C, 16 h (yield: 77%, 83%, and 74%); (iv) Ac_2O , 75 °C, 4 h (yield: 76%); (v) $MeNH_2$ (33 wt % in EtOH), THF, 0 °C \rightarrow RT, 16 h (yield: 83%); (vi) NaOAc, Ac_2O , 90 °C, 16 h (yield: 93%); (vii) NBS, TFA/conc H_2SO_4 (3:1, v/v), RT, 16 h (yield: 83%).

(possibly from homocoupling between IDT units) of less than 5% (Figure S3 and Table S1).

Optoelectronic Properties. The steady-state ultraviolet and visible light (UV-vis) and photoluminescence (PL) spectroscopies for the polymers are depicted in Figure 2, and several extracted parameters are listed in Table 1. From the

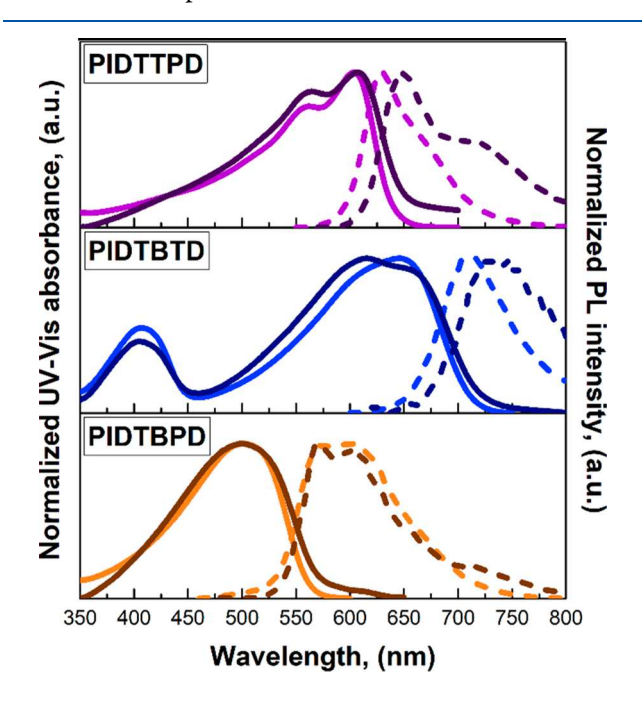


Figure 2. UV-vis (solid lines) and PL (dashed lines) spectra for solution (lighter color) and thin film (darker color) of the polymers.

UV-vis spectra, PIDTTPD exhibits an absorption maximum around 605 nm in solution which remains unchanged in the thin film. Compared with PIDTTPD, the absorption maxima of PIDTBTD are at longer wavelengths (645 nm in solution and 615 nm in the thin film). This is attributed to a stronger acceptor strength of BTD compared to TPD, a claim supported by the larger Stokes shift (71 nm for solution and 110 nm for thin film) observed in the PL spectra of PIDTBTD. A larger Stokes shift is often seen with increasing acceptor strength in donor-acceptor compounds with the same donor unit.³⁴ The blue-shifted absorption maxima of PIDTBPD with respect to the other polymers is due to the twist in the backbone of PIDTBPD, as supported by DFT, which significantly reduces the effective conjugation length of the polymer. From solution to thin film, the minimal shift observed in absorption spectra indicates that all polymers undergo minimal conformational change, implying weak solid-state intermolecular interactions, a property ascribed to the long alkyl side chains on the bridging $C(sp^3)$, as well as the twisted polymer backbone in the case of PIDTBPD. The observed absorption shoulder in the thin film UV-vis of PIDTTPD and PIDTBTD suggests some polymer aggregation in the thin film. This also indicates that although the intermolecular interactions for all of three polymers are weak, the intermolecular interactions of PIDTTPD and PIDTBTD are stronger than that of PIDTBPD. This assertion about weak intermolecular interactions is also supported by PL spectra of these polymers. The unchanged PL spectrum from solution to thin film implies that polymer chain behaves individually. The lack of observable change in the solution and thin-film PL of PIDTBPD implies that it possesses the weakest intermolecular interaction among the three polymers.

Crystallinity and Thermal Stability. The glass transition temperature $(T_{\rm g})$ is a critical parameter related to the polymer's mechanical properties. Differential scanning calorimetry (DSC) was used to determine the $T_{\rm g}$ of these alkyl-IDT polymers. Before the DSC measurements, thermogravimetric analysis (TGA) was performed to ensure that no moisture or residual solvent was contained in these polymers, which would potentially act as a plasticizer and artificially soften the polymers. The TGA results also indicate that the polymers are thermally stable up to 390 °C (Figure S4a). As shown in Table 1, all polymers possess $T_{\rm g}$ below room temperature (Figure S4b). Finally, no apparent melting or crystallization peaks were observed for these polymers, indicating a low degree of crystallinity in the solid state.

Polymer Chain Packing. X-ray diffraction (XRD) measurements were conducted to investigate the thin film microstructures of these alkyl-IDT polymers. Experiments were conducted on polymer films before and after annealing at 200 °C. The results are depicted in Figure 3. The diffraction peak at $2\theta = 3.7^{\circ}$ represents the edge-on packing, with a dspacing of 23.9 Å, and the diffraction peak at $2\theta = 20^{\circ}$ corresponds to π -stacking, with a d-spacing of 4.4 Å. All polymers exhibit the same broad $2\theta = 20^{\circ}$ diffraction peaks before and after annealing, indicating weak π -stacking and short coherence lengths in the π -stacking direction. The intensity change in the $2\theta = 3.7^{\circ}$ peak after annealing is 3% and 12% for PIDTTPD and PIDTBTD, respectively, which are both relatively minor changes (Table 1). This implies stable polymer packing in this direction. However, significant instability is observed for PIDTBPD, with its $2\theta = 3.7^{\circ}$ peak intensity decreasing by 51% upon annealing (Table 1). This

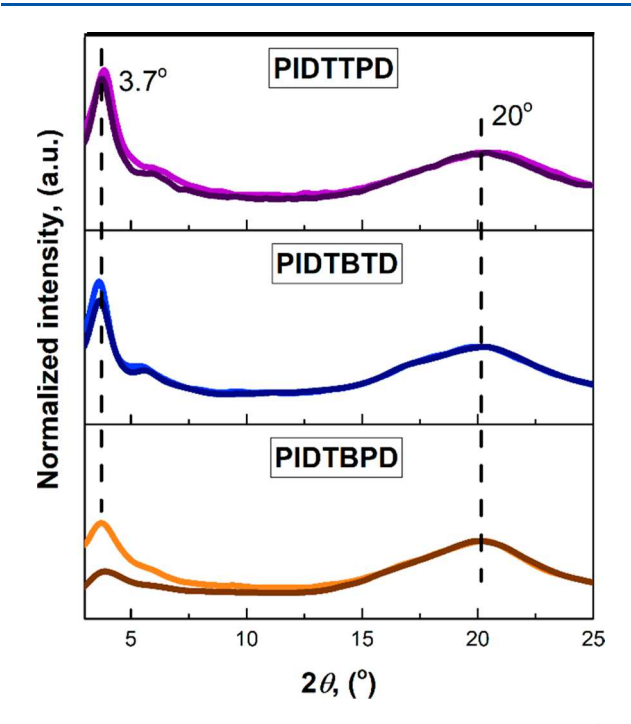


Figure 3. XRD results of the thin films of the polymers before (light color) and after annealing (dark color).

also supports the notion that PIDTBPD possesses the weakest intermolecular interactions among the polymers. In addition to the XRD measurements, the absorption spectra of the polymer thin films were also measured at different annealing temperatures to support the claim that the intermolecular interactions of PIDTBPD is weaker than that of PIDTTPD and PIDTBTD (Figure S5). The 0-0 and 0-1 characteristic peaks of PIDTTPD did not undergo apparent change when the annealing temperature was between 40 to 200 °C and compared with the spectrum measured at room temperature (Figure S5a and Figure 2). The 0-0 and 0-1 peaks of PIDTBTD appears under annealing suggestive of the formation of an ordered polymer chain packing driven by thermal force. The same observation can be made for PIDTBPD. However, the 0-1 peak appears only when the annealing temperature raised from 40 °C to 80 and 120 °C. Further increasing the annealing temperature to 160 and 200 °C induces the disappearance of the 0-1 peak, indicating that the polymer chain packing becomes disordered again.

Charge Transport Properties. The charge transport properties of the alkyl-IDT polymers were studied using OFETs with a bottom-gate top-contact architecture (Figure S6). It was found that all polymers exhibited p-type behavior with a gate bias sweep from 0 to -100 V and a drain bias of −100 V. Under these saturation conditions, the linear regime of the square root of the drain-source current $(I_{DS}^{1/2})$ vs gate voltage (V_G) curve (eq S1 and Figure S7) corresponded to a hole mobility (μ) of varying from 0.06 to 0.20 cm² V⁻¹ s⁻¹ and a source-drain current on/off ratio (I_{on}/I_{off}) ranging from 2 × 10^4 to 3×10^6 for these polymers (Table 1). The devices were also tested for ambipolar properties by setting the drain bias to +100 V and sweeping the gate bias from 0 to +100 V. Each of the polymers displayed negligible current flow under this ntype configuration. The charge mobility of these polymers is slightly higher than that of spin-coated P3HT ($\mu = 0.075 \pm$ 0.013 cm² V⁻¹ s⁻¹, measured in our lab using the same device

architecture as this report, Table S2) and ranks relatively high compared to other semiconducting copolymers that have also been tested for mechanical properties.²⁴ The charge mobility of these polymers follows the general trend that increased backbone planarity leads to increased charge mobility (Table 1).

Mechanical Properties. The mechanical properties of the alkyl-IDT polymers were measured on thin-film samples. These properties are quantified by two parameters: $E_{\rm f}$ and CoS. The former represents the polymer's stiffness while the latter is related to the polymer's ductility. A buckling-based metrology was used to determine the elastic moduli of the alkyl-IDT polymers. The CoS is determined as the strain at which fractures are first observed in the polymer film using optical microscopy. Experimental details are given in the Supporting Information (Figure S8 and Table S3).

It should be noted that all polymers exhibit low $E_{\rm f}$ values of less than 450 MPa (Table 1). This is far below that of poly(3hexylthiophene) (P3HT), a widely studied semiconducting homopolymer that is quite stiff $(E_f = 1000-1100 \text{ MPa})^{.37}$ Compared to other semiconducting copolymers ($E_f = 300$ – 1500 MPa), the elastic moduli of these polymers are also quite low.²³ This is attributed to the long alkyl side chains in these polymers, which exhibit a large degree of freedom and increases the excluded volume of these side chains. This is supported by a recent study of the mechanical properties of conjugated polymers, showing that elastic modulus decreases with increasing length of the alkyl side chains, from 1870 MPa for butyl side chains to 160 MPa for dodecyl chains in poly(3alkylthiophenes).³⁸ The increased excluded volume decreases the volume fraction of the backbone chains, reducing the loadbearing carbon content. Additionally, this large excluded volume contributes to the weak π -stacking as observed in the XRD patterns of these polymers. It is reasonable to think that the intermolecular interactions from the side-chain interactions dominate the elastic modulus of these alkyl-IDT polymers.

Though these polymers exhibit similar elastic moduli, their crack-onset strain varies dramatically (Table 1). PIDTTPD and PIDTBTD exhibit brittle behavior (CoS = 3%), which are similar to typical semiconducting copolymers (CoS < 15%)²³ and P3HT (CoS = 5-9%),³⁸ while PIDTBPD exhibited highly ductile behavior, beyond the limit of the measurement apparatus (CoS > 100%). Polymer deformation mechanisms are extremely complex; however, it is clear that the reduction in interchain interactions along the π -stacking direction has a dramatic effect on the maximum elongation.

Morphological Studies. To study the effect of the mechanical properties of the polymers on charge mobility, the best way is to fabricate stretchable OFETs using the polymers and measure the charge mobility under different mechanical deformations. To this end, we choose to fabricate stretchable OFETs on polydimethylsiloxane (PDMS) substrates according to literature procedures. ^{40–42} However, the attempt was not successful because we found that polymers exhibit poor compatibility with PDMS (Figure S9), and as a result most fabricated devices failed to work. For the working devices, we found a very low current between source and drain possibly due to the poor compatibility between the polymers and dielectric layers, which significantly suppressed charge injection (Table S4). It is well-known that the electronic performance of polymers are correlated to the surface morphology of the thin film. To this end, we performed morphological studies on polymer thin films under different

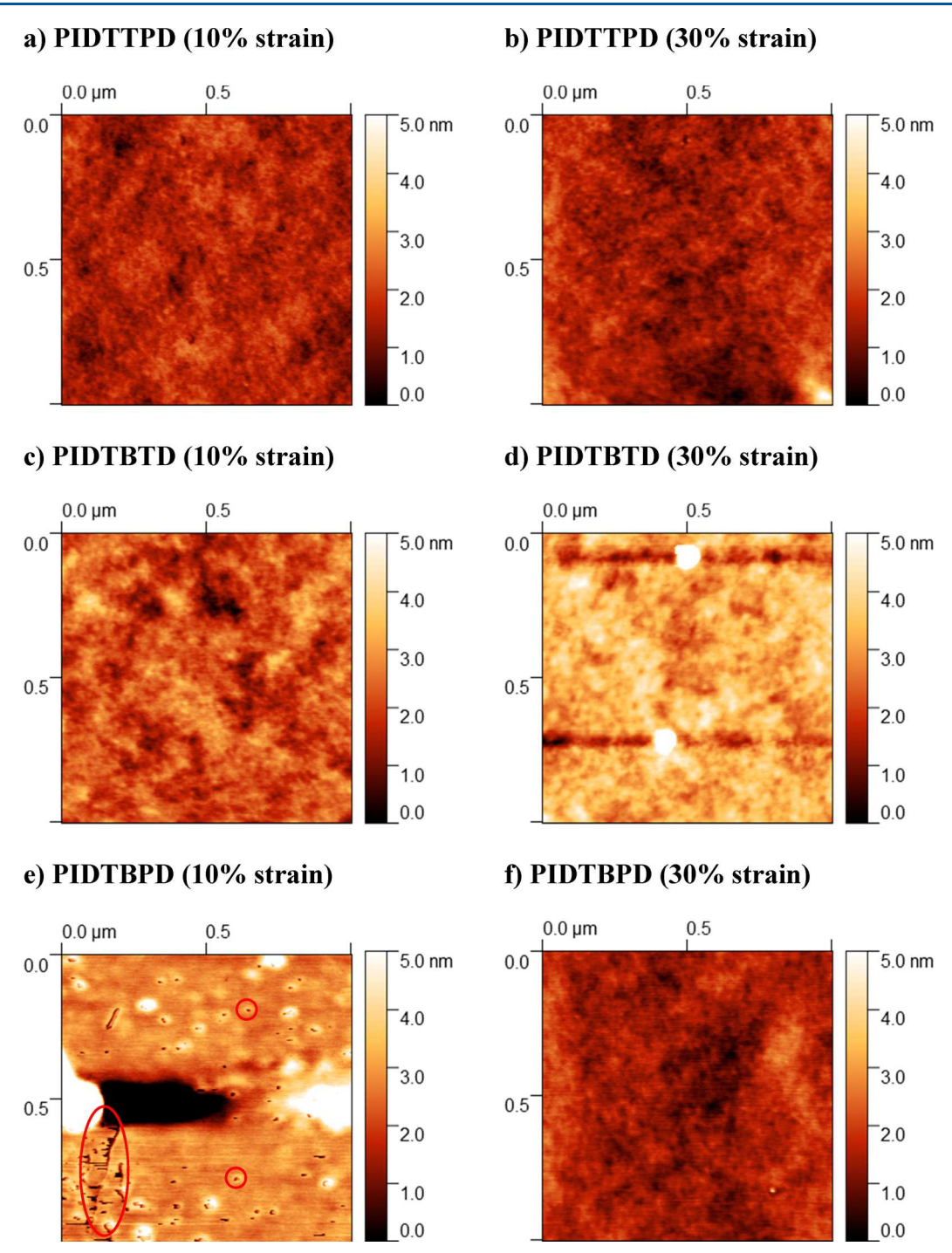


Figure 4. Surface morphologies of the polymers under different strains obtained using contact mode AFM (bright spots are dust particles on the film).

strains (10% and 30%) by atomic force microscopy (AFM). The stretched polymer thin films were prepared by transferring the spin-coated polymer thin films (10 mg/mL) on glass substrate (precoated with PEDOT:PSS) to paraffin films (Parafilm). The purpose is to achieve permanent deformation of the polymer thin films. The surface morphologies of the stretched polymer thin films are depicted in Figure 4. It is noted that different from the CoS measurements that PIDTTPD and PIDTBTD exhibited only 3% CoS values, both polymers did not show any cracks in the surface images (Figure 4a-d). This is possibly because a much thinner polymer films were prepared in the experiments (in CoS

measurements, the polymer thin films were prepared from 30 mg/mL solution) and because the CoS measurements were performed on PDMS. Additionally, associated with the highly deformable feature of Parafilm, the polymers could exhibit nanoconfinement effect that boosts the stretchability of the polymer thin films. When the polymer thin films were stretched from 10% strain to 30% strain, the root-mean-square (rms) surface roughness increased slightly for PIDTTPD and PIDTBTD. Specifically, the rms surface roughness of PIDTTPD thin film increased from 0.33 to 0.45 nm while for PIDTBTD thin film it increased from 0.52 to 0.62 nm. As of PIDTBPD, it behaved slightly differently from the other two

polymers. First, scrapes (large red oval) and pinholes (small red circles) were observed (Figure 4e) in the polymer thin film under 10% strain. The scrapes and pinholes were caused by AFM tips interacting with the polymer thin film during the measurements, which indicate that the polymer thin film surface is soft. The rms surface roughness was 0.37 nm excluding the scrapes and pinholes. At 30% strain, the rms surface roughness was 0.40 nm. The thin scrapes are still visible from along the scan axis (left to right). Excluding the scrapes and pinholes, there are also no observable cracks in the PIDTBPD thin films. Experiments on PIDTBPD thin film are consistent with the results obtained from mechanical measurements. The changes in rms surface roughness and morphology for all polymer thin films are very small, and it is reasonable to believe that if stretchable OFETs were fabricated, the charge mobility would not exhibit a significant decrease when the devices are under strain.

CONCLUSIONS

In summary, a series of alkyl-IDT polymers were designed with increasing backbone twist, as supported by DFT calculations. They were then synthesized via DArP. UV-vis and PL measurements suggest weak intermolecular interactions among these polymers, with PIDTBPD being the weakest due to the highly kinked backbone. These polymers possess T_g below room temperature, and their XRD patterns indicate low crystallinity. Their charge mobilities are relatively high (μ = 0.06-0.20 cm² V⁻¹ s⁻¹) with increased backbone planarity leading to increased charge mobility. These polymers exhibit low elastic moduli (E_f < 450 MPa), a feature dominated by the presence of the long, linear alkyl side chains. PIDTTPD and PIDTBTD have planar backbones and correspondingly exhibit brittle behavior with crack-onset strains of 3%, while PIDTBPD has a kinked backbone and exhibits high ductility (CoS > 100%). Intermolecular interactions seem to suppress polymer ductility, suggesting that the low intermolecular interactions of the PIDTBPD, which stem from its kinked backbone, are responsible for the high ductility. No observable changes were found in polymer thin films under different strains in surface morphological studies, implying that minimal effect on charge mobilities of the polymers if the stretchable devices were fabricated. The work presented here allows one to deduce several structure-property relationships that will enable the design of high-mobility, low-stiffness, and largeductility semiconducting polymers.

ASSOCIATED CONTENT

S Supporting Information

The Supporting Information is available free of charge on the ACS Publications website at DOI: 10.1021/acs.macromol.8b00898.

Experimental details, figures and tables, and compound characterization data (PDF)

AUTHOR INFORMATION

Corresponding Author

*E-mail: luscombe@uw.edu (C.K.L.).

ORCID ®

Christine K. Luscombe: 0000-0001-7456-1343

Notes

The authors declare no competing financial interest.

ACKNOWLEDGMENTS

This work was supported by the NSF under the CCI Center for Selective C-H Functionalization (CHE-1700982), DMR-1533372, and DMR-1708317. It was also in part supported by the State of Washington through the University of Washington Clean Energy Institute (J.W.O.) and NSF NRT-DESE 1633216 (W.K.T.). Part of this work was conducted at the Washington Nano Fabrication Facility/Molecular Analysis Facility, a National Nanotechnology Coordinated Infrastructure (NNCI) site at the University of Washington, which is supported in part by funds from the National Science Foundation (Grants 1542101, 1337840, and 0335765), the National Institutes of Health, the Molecular Engineering & Sciences Institute, the Clean Energy Institute, the Washington Research Foundation, the M. J. Murdock Charitable Trust, Altatech, ClassOne Technology, GCE Market, Google, and SPTS.

REFERENCES

- (1) Holliday, S.; Li, Y.; Luscombe, C. K. Recent Advances in High Performance Donor-Acceptor Polymers for Organic Photovoltaics. *Prog. Polym. Sci.* **2017**, *70*, 34–51.
- (2) Torsi, L.; Magliulo, M.; Manoli, K.; Palazzo, G. Organic Field-Effect Transistor Sensors: A Tutorial Review. *Chem. Soc. Rev.* **2013**, 42 (22), 8612–8628.
- (3) Geffroy, B.; le Roy, P.; Prat, C. Organic Light-Emitting Diode (OLED) Technology: Materials, Devices and Display Technologies. *Polym. Int.* **2006**, 55 (6), 572–582.
- (4) Russ, B.; Glaudell, A.; Urban, J. J.; Chabinyc, M. L.; Segalman, R. A. Organic Thermoelectric Materials for Energy Harvesting and Temperature Control. *Nat. Rev. Mater.* **2016**, *1*, 16050.
- (5) Kim, D. H.; Lu, N. S.; Ma, R.; Kim, Y. S.; Kim, R. H.; Wang, S. D.; Wu, J.; Won, S. M.; Tao, H.; Islam, A.; Yu, K. J.; Kim, T. I.; Chowdhury, R.; Ying, M.; Xu, L. Z.; Li, M.; Chung, H. J.; Keum, H.; McCormick, M.; Liu, P.; Zhang, Y. W.; Omenetto, F. G.; Huang, Y. G.; Coleman, T.; Rogers, J. A. Epidermal Electronics. *Science* 2011, 333 (6044), 838–843.
- (6) Kim, D. H.; Lu, N. S.; Ghaffari, R.; Kim, Y. S.; Lee, S. P.; Xu, L. Z.; Wu, J. A.; Kim, R. H.; Song, J. Z.; Liu, Z. J.; Viventi, J.; de Graff, B.; Elolampi, B.; Mansour, M.; Slepian, M. J.; Hwang, S.; Moss, J. D.; Won, S. M.; Huang, Y. G.; Litt, B.; Rogers, J. A. Materials For Multifunctional Balloon Catheters with Capabilities in Cardiac Electrophysiological Mapping and Ablation Therapy. *Nat. Mater.* **2011**, *10* (4), 316–323.
- (7) Tee, B. C. K.; Chortos, A.; Berndt, A.; Nguyen, A. K.; Tom, A.; McGuire, A.; Lin, Z. L. C.; Tien, K.; Bae, W. G.; Wang, H. L.; Mei, P.; Chou, H. H.; Cui, B. X.; Deisseroth, K.; Ng, T. N.; Bao, Z. N. A Skin-Inspired Organic Digital Mechanoreceptor. *Science* **2015**, *350* (6258), 313–316.
- (8) Kaltenbrunner, M.; Sekitani, T.; Reeder, J.; Yokota, T.; Kuribara, K.; Tokuhara, T.; Drack, M.; Schwodiauer, R.; Graz, I.; Bauer-Gogonea, S.; Bauer, S.; Someya, T. An Ultra-Lightweight Design for Imperceptible Plastic Electronics. *Nature* **2013**, 499 (7459), 458–463.
- (9) Sun, Y. G.; Choi, W. M.; Jiang, H. Q.; Huang, Y. G. Y.; Rogers, J. A. Controlled Buckling of Semiconductor Nanoribbons for Stretchable Electronics. *Nat. Nanotechnol.* **2006**, *1* (3), 201–207.
- (10) Shyu, T. C.; Damasceno, P. F.; Dodd, P. M.; Lamoureux, A.; Xu, L. Z.; Shlian, M.; Shtein, M.; Glotzer, S. C.; Kotov, N. A. A Kirigami Approach to Engineering Elasticity in Nanocomposites through Patterned Defects. *Nat. Mater.* **2015**, *14* (8), 785–789.
- (11) McCoul, D.; Hu, W. L.; Gao, M. M.; Mehta, V.; Pei, Q. B. Recent Advances in Stretchable and Transparent Electronic Materials. *Adv. Electron. Mater.* **2016**, 2 (5), 1500407.
- (12) Trung, T. Q.; Lee, N. E. Recent Progress on Stretchable Electronic Devices with Intrinsically Stretchable Components. *Adv. Mater.* **2017**, 29 (3), 1603167.

(13) Oh, J. Y.; Rondeau-Gagne, S.; Chiu, Y. C.; Chortos, A.; Lissel, F.; Wang, G. J. N.; Schroeder, B. C.; Kurosawa, T.; Lopez, J.; Katsumata, T.; Xu, J.; Zhu, C. X.; Gu, X. D.; Bae, W. G.; Kim, Y.; Jin, L. H.; Chung, J. W.; Tok, J. B. H.; Bao, Z. N. Intrinsically Stretchable and Healable Semiconducting Polymer for Organic Transistors. *Nature* 2016, 539 (7629), 411–415.

- (14) Xu, J.; Wang, S. H.; Wang, G. J. N.; Zhu, C. X.; Luo, S. C.; Jin, L. H.; Gu, X. D.; Chen, S. C.; Feig, V. R.; To, J. W. F.; Rondeau-Gagne, S.; Park, J.; Schroeder, B. C.; Lu, C.; Oh, J. Y.; Wang, Y. M.; Kim, Y. H.; Yan, H.; Sinclair, R.; Zhou, D. S.; Xue, G.; Murmann, B.; Linder, C.; Cai, W.; Tok, J. B. H.; Chung, J. W.; Bao, Z. N. Highly Stretchable Polymer Semiconductor Films through the Nanoconfinement Effect. *Science* 2017, 355 (6320), 59–64.
- (15) Kim, H. J.; Thukral, A.; Yu, C. J. Highly Sensitive and Very Stretchable Strain Sensor Based on a Rubbery Semiconductor. ACS Appl. Mater. Interfaces 2018, 10 (5), 5000–5006.
- (16) Wu, H.-C.; Benight, S. J.; Chortos, A.; Lee, W.-Y.; Mei, J.; To, J. W. F.; Lu, C.; He, M.; Tok, J. B.-H.; Chen, W.-C.; Bao, Z. A Rapid and Facile Soft Contact Lamination Method: Evaluation of Polymer Semiconductors for Stretchable Transistors. *Chem. Mater.* **2014**, *26* (15), 4544–4551.
- (17) Li, Y.; Tatum, W. K.; Onorato, J. W.; Barajas, S. D.; Yang, Y. Y.; Luscombe, C. K. An Indacenodithiophene-Based Semiconducting Polymer with High Ductility for Stretchable Organic Electronics. *Polym. Chem.* **2017**, *8* (34), 5185–5193.
- (18) Wu, H.-C.; Hung, C.-C.; Hong, C.-W.; Sun, H.-S.; Yamashita, J.-T. W. G.; Higashihara, T.; Chen, W.-C. Isoindigo-Based Semiconducting Polymers Using Carbosilane Side Chains for High Performance Stretchable Field-Effect Transistors. *Macromolecules* **2016**, 49 (22), 8540–8548.
- (19) Wen, H.-F.; Wu, H.-C.; Aimi, J.; Hung, C.-C.; Chiang, Y.-C.; Kuo, C.-C.; Chen, W.-C. Soft Poly(butyl acrylate) Side Chains toward Intrinsically Stretchable Polymeric Semiconductors for Field-Effect Transistor Applications. *Macromolecules* **2017**, *50* (13), 4982–4992.
- (20) Zhao, Y.; Zhao, X.; Zang, Y.; Di, C.-A.; Diao, Y.; Mei, J. Conjugation-Break Spacers in Semiconducting Polymers: Impact on Polymer Processability and Charge Transport Properties. *Macromolecules* **2015**, *48* (7), 2048–2053.
- (21) Printz, A. D.; Savagatrup, S.; Burke, D. J.; Purdy, T. N.; Lipomi, D. J. Increased Elasticity of a Low-Bandgap Conjugated Copolymer by Random Segmentation for Mechanically Robust Solar Cells. *RSC Adv.* **2014**, *4* (26), 13635–13643.
- (22) Son, S. Y.; Kim, J. H.; Song, E.; Choi, K.; Lee, J.; Cho, K.; Kim, T. S.; Park, T. Exploiting pi-pi Stacking for Stretchable Semi-conducting Polymers. *Macromolecules* **2018**, *51* (7), 2572–2579.
- (23) Roth, B.; Savagatrup, S.; de los Santos, N. V.; Hagemann, O.; Carle, J. E.; Helgesen, M.; Livi, F.; Bundgaard, E.; Sondergaard, R. R.; Krebs, F. C.; Lipomi, D. J. Mechanical Properties of A Library of Low-Band-Gap Polymers. *Chem. Mater.* **2016**, 28 (7), 2363–2373.
- (24) Onorato, J.; Pakhnyuk, V.; Luscombe, C. K. Structure and Design of Polymers for Durable, Stretchable Organic Electronics. *Polym. J.* **2017**, *49*, 41–60.
- (25) Noriega, R.; Rivnay, J.; Vandewal, K.; Koch, F. P. V.; Stingelin, N.; Smith, P.; Toney, M. F.; Salleo, A. A General Relationship between Disorder, Aggregation and Charge Transport in Conjugated Polymers. *Nat. Mater.* **2013**, *12*, 1038–1044.
- (26) Zhang, W.; Smith, J.; Watkins, S. E.; Gysel, R.; McGehee, M.; Salleo, A.; Kirkpatrick, J.; Ashraf, S.; Anthopoulos, T.; Heeney, M.; McCulloch, I. Indacenodithiophene Semiconducting Polymers for High-Performance, Air-Stable Transistors. *J. Am. Chem. Soc.* **2010**, 132 (33), 11437—9.
- (27) Zhong, W.; Sun, S.; Ying, L.; Liu, F.; Lan, L.; Huang, F.; Cao, Y. High-Performance Organic Field-Effect Transistors Fabricated Based on a Novel Ternary π-Conjugated Copolymer. ACS Appl. Mater. Interfaces 2017, 9 (8), 7315–7321.
- (28) Zhang, X.; Bronstein, H.; Kronemeijer, A. J.; Smith, J.; Kim, Y.; Kline, R. J.; Richter, L. J.; Anthopoulos, T. D.; Sirringhaus, H.; Song, K.; Heeney, M.; Zhang, W.; McCulloch, I.; DeLongchamp, D. M. Molecular Origin of High Field-Effect Mobility in An Indacenodi-

thiophene-Benzothiadiazole Copolymer. Nat. Commun. 2013, 4, 2238.

- (29) McCormick, T. M.; Bridges, C. R.; Carrera, E. I.; Di Carmine, P. M.; Gibson, G. L.; Hollinger, J.; Kozycz, L. M.; Seferos, D. S. Conjugated Polymers: Evaluating DFT Methods for More Accurate Orbital Energy Modeling. *Macromolecules* **2013**, *46* (10), 3879–3886.
- (30) Tam, T. L. D.; Lin, T. T. Tuning Energy Levels and Film Morphology in Benzodithiophene—Thienopyrrolodione Copolymers via Nitrogen Substitutions. *Macromolecules* **2016**, *49* (5), 1648–1654.
- (31) Okamoto, K.; Zhang, J. X.; Housekeeper, J. B.; Marder, S. R.; Luscombe, C. K. C-H Arylation Reaction: Atom Efficient and Greener Syntheses of pi-Conjugated Small Molecules and Macromolecules for Organic Electronic Materials. *Macromolecules* **2013**, 46 (20), 8059–8078.
- (32) Suraru, S.-L.; Lee, J. A.; Luscombe, C. K. C–H Arylation In The Synthesis Of Π-Conjugated Polymers. *ACS Macro Lett.* **2016**, *5* (6), 724–729.
- (33) Wang, X.; Wang, M. Synthesis of Donor-Acceptor Conjugated Polymers based on Benzo[1,2-b:4,5-b']dithiophene and 2,1,3-Benzothiadiazole via Direct Arylation Polycondensation: Towards Efficient C—H Activation in Nonpolar Solvents. *Polym. Chem.* **2014**, 5, 5784—5792.
- (34) Li, Y.; Ren, T. H.; Dong, W. J. Tuning Photophysical Properties of Triphenylamine and Aromatic Cyano Conjugate-based Wavelength-Shifting Compounds by Manipulating Intramolecular Charge Transfer Strength. J. Photochem. Photobiol., A 2013, 251, 1–9.
- (35) Levine, H.; Slade, L. 2-Water As A Plasticizer: Physico-Chemical Aspects of Low-Moisture Polymeric Systems; Cambridge University Press: 1988; pp 79–185.
- (36) Stafford, C. M.; Harrison, C.; Beers, K. L.; Karim, A.; Amis, E. J.; VanLandingham, M. R.; Kim, H. C.; Volksen, W.; Miller, R. D.; Simonyi, E. E. A Buckling-Based Metrology For Measuring The Elastic Moduli Of Polymeric Thin Films. *Nat. Mater.* **2004**, 3 (8), 545–50.
- (37) Tahk, D.; Lee, H. H.; Khang, D.-Y. Elastic Moduli of Organic Electronic Materials by the Buckling Method. *Macromolecules* **2009**, 42 (18), 7079–7083.
- (38) Savagatrup, S.; Makaram, A. S.; Burke, D. J.; Lipomi, D. J. Mechanical Properties of Conjugated Polymers and Polymer-Fullerene Composites as A Function of Molecular Structure. *Adv. Funct. Mater.* **2014**, *24* (8), 1169–1181.
- (39) Savagatrup, S.; Printz, A. D.; O'Connor, T. F.; Zaretski, A. V.; Rodriquez, D.; Sawyer, E. J.; Rajan, K. M.; Acosta, R. I.; Root, S. E.; Lipomi, D. J. Mechanical Degradation and Stability of Organic Solar Cells: Molecular and Microstructural Determinants. *Energy Environ. Sci.* **2015**, *8*, 55–80.
- (40) Lei, T.; Guan, M.; Liu, J.; Lin, H. C.; Pfattner, R.; Shaw, L.; McGuire, A. F.; Huang, T. C.; Shao, L.; Cheng, K. T.; Tok, J. B.; Bao, Z. Biocompatible and Totally Disintegrable Semiconducting Polymer for Ultrathin and Ultralightweight Transient Electronics. *Proc. Natl. Acad. Sci. U. S. A.* **2017**, *114* (20), 5107–5112.
- (41) Kim, H. J.; Sim, K.; Thukral, A.; Yu, C. J. Rubbery Electronics and Sensors from Intrinsically Stretchable Elastomeric Composites of Semiconductors and Conductors. *Sci. Adv.* **2017**, *3* (9), e1701114.
- (42) Chortos, A.; Lim, J.; To, J. W. F.; Vosgueritchian, M.; Dusseault, T. J.; Kim, T. H.; Hwang, S.; Bao, Z. A. Highly Stretchable Transistors Using a Microcracked Organic Semiconductor. *Adv. Mater.* **2014**, *26* (25), 4253–4259.